

VERTICAL CASCADED PLANAR EBG STRUCTURE FOR SSN SUPPRESSION

Ling-Feng Shi^{1, 2, *} and Hong-Feng Jiang^{1, 2}

¹Key Lab of High-Speed Circuit Design and EMC, Ministry of Education, Xidian University, Xi'an, Shaanxi 710071, China

²Institute of Electronic CAD, Xidian University, Xi'an, Shaanxi 710071, China

Abstract—A novel vertical cascaded planar electromagnetic bandgap (EBG) structure is proposed for SSN suppression with the ultra-wideband at the restraining depth of -30 dB by analyzing the simultaneous switching noise (SSN) suppression mechanism and the equivalent circuit model for EBG structure. Moreover, the SSN suppression bandwidth can be broadened by using different novel EBG structures required by vertically cascading different planar EBG structures. In addition, the structure is verified to meet signal integrity (SI) by the time-domain simulation. The tested results show that the presented EBG is accordant to the simulated results of the theory method by the vector network analyzer. The proposed structures provide a new designing method for EBG structures to improve the ability of suppressing SSN.

1. INTRODUCTION

With the development of fast edge rates and high clock frequencies, simultaneous switching noise (SSN) has become one of the major concerns for the high-speed digital circuits. SSN known as power/ground bounce noise or delta-I noise mainly attributes to three reasons, namely mutual inductive coupling of power distribution networks (PDN), inductance of non-ideal signal path and power supply compression. The SSN leads to the cavity resonance modes within the parallel-plate waveguide-type power/ground planes. The resonance modes among the power and ground planes cause serious signal

Received 1 August 2013, Accepted 28 August 2013, Scheduled 11 September 2013

* Corresponding author: Ling-Feng Shi (slf-good@163.com).

integrity (SI) or power integrity (PI) problems for the high-speed circuits [1–3].

In recent years, there are many approaches to solve these problems. Adding decoupling capacitors, selecting the number and location of the vias and using differential interconnection can effectively suppress SSN [4]. However, these methods have some deficiencies. Adding decoupling capacitors is suitable for high frequency. However, it is difficult to determine the number and location of vias. Using differential interconnections costs too much. So it is necessary to find some more effective ways to deal with the SSN.

Electromagnetic bandgap (EBG) structure derived from the photonic bandgap (PBG) structure is a kind of periodic unit composed of metal and dielectric [5]. Because of the electromagnetic properties, EBG structures lead to a wide range of applications for the filter [6, 7] and antenna [8, 9]. Most recently, a novel concept using EBG structure is introduced to suppress the SSN. Various EBG structures have been proposed to offer an alternative solution in the SSN suppression. For example, mushroom-like EBG structure [4] and 3-D cascaded mushroom EBG [10] can be used to reduce SSN, but it leads to the increased cost in print circuit board (PCB). However, the planar EBG structures are suitable for a low-cost design and also adapted to suppress SSN [11–14], such as L-bridge structure, meander-L structure and π -bridge structure. But the bandwidth of these structures is limited. At present, some researchers have embedded EBG structure between two layers of ground to get a better suppression solution [15–17]. Although the effect has been improved, it does not achieve the capability of the ultra-wideband SSN suppression.

A novel vertical cascaded planar EBG structure is proposed in this paper. It makes two planar EBG structures achieve vertical cascade using the vias to get better SSN suppression effect on the basis of previous work. Simultaneously, the SSN suppression bandwidth can be broadened by using the different novel EBG structures required by vertically cascading planar EBG with different structures. Finally, the simulated results of the proposed EBG are the same as the tested ones, and time-domain simulation results show that the novel EBG structure in high-speed circuits can meet the requirement for SI.

2. STRUCTURE DESIGN

2.1. Novel Vertical Cascaded Planar EBG Structure

Figure 1(a) shows the previous L-bridge EBG power/ground planes design. The ground plane is kept continuous, and the power plane is

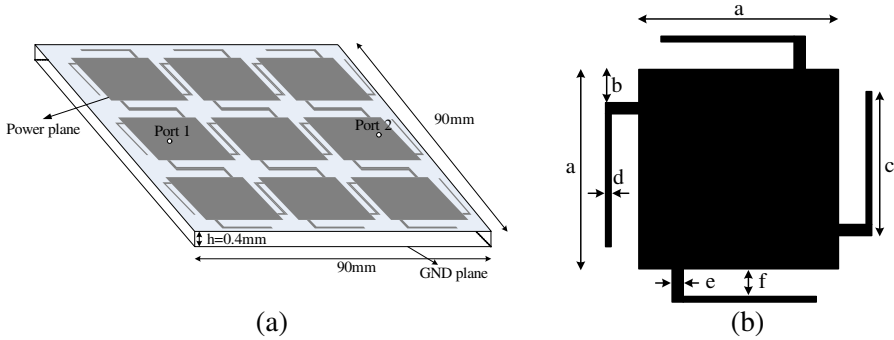


Figure 1. The L-bridge EBG test prototype and the unit cell dimensions. (a) 3D view and the locations of two ports. (b) Parameters of a square unit cell.

etched to nine cells EBG with L-shaped bridges. The unit cell of the L-bridge EBG is shown in Figure 1(b). The corresponding parameter is set to $a = 30\text{ mm}$, $b = 7.5\text{ mm}$, $c = 15.2\text{ mm}$, $d = 0.1\text{ mm}$, $e = 0.2\text{ mm}$, $f = 0.55\text{ mm}$. The simulated and measured results have demonstrated that the SSN can be suppressed with the wideband from 600 MHz to 4.6 GHz at the restraining depth of -30 dB [11]. However, it is a narrow bandwidth.

Based on [11], a new vertical cascaded planar EBG structure is proposed. As shown in Figure 2(a), the perpendicular cascade is achieved by inserting two L-bridge EBG structures together. The new EBG structure is shown in Figure 2(b). The structure is divided into four layers for the power plane, ground plane, ground plane and power plane, respectively. The distance between the layers is 0.1 mm, 0.3 mm and 0.1 mm from the top to the bottom. Nine-cell EBG with L-shaped bridges are etched on the power plane. There are nine vias used to connect the two power planes together to form the vertical cascaded structure. The radius of the through hole is 0.2 mm. The square unit cell is shown in Figure 2(c).

2.2. The Simulation and Measurement Result

To verify the effectiveness, a design of four-layer PCB with the dimension $90 \times 90 \times 0.5\text{ mm}^3$ consisting of 3×3 unit cells is shown in Figure 3. The substrate dielectric is FR4 with a relative permittivity of 4.4 and a loss tangent of 0.02. S -parameter is generally used to test the ability of SSN suppression. The model in Figure 3(a) is established with HFSS software. Three ports are located at port-1 (7.5 mm, 45 mm,

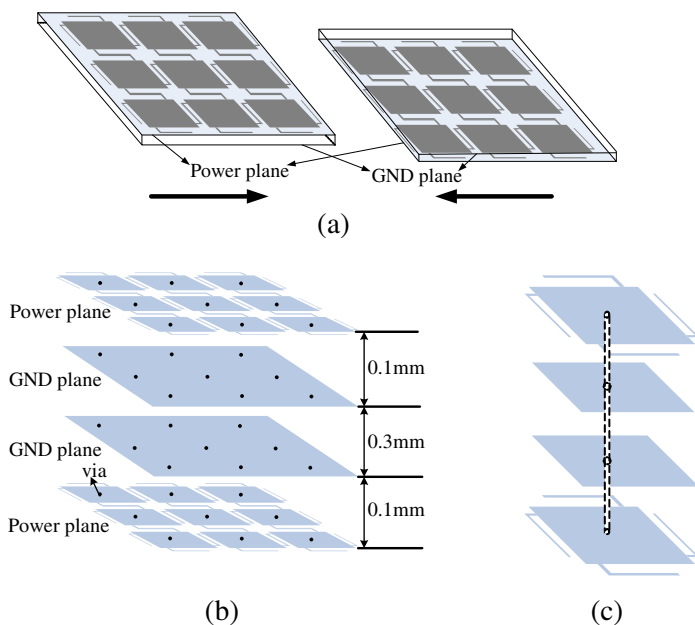


Figure 2. The novel vertical cascaded planar EBG structure. (a) The two L-bridge EBG interspersed cascade way. (b) The lateral view of novel EBG structure. (c) The showing of square unit cell.

0 mm), port-2 (82.5 mm, 45 mm, 0 mm) and port-3 (45 mm, 7.5 mm, -0.5 mm). Port-1 plays the role of input, while the others are output ports. The real PCB for the novel vertical cascaded planar EBG design is shown in Figure 3(b).

Figure 4 shows the simulated and measured S -parameters for the designed novel vertical cascaded planar EBG structure and L-bridge EBG structure. As shown in Figure 4(a), designed structure possesses a good performance. The SSN suppression is observed starting at approximately 710 MHz and extending to 10 GHz at -30 dB suppression of the bandgap depth. But the L-bridge EBG only has 4 GHz bandwidth. So the new structure has met the requirement of ultra-wideband capability. Simultaneously, the simulated result is similar to the measurement one as shown in Figure 4 by the vector network analyzer (VNA). Meanwhile, as can be seen in Figure 4(b), the measurements of both S_{21} and S_{31} have good ultra-wideband SSN suppression at the restraining depth of -30 dB. It is shown that the novel vertical cascaded planar EBG structure has a good performance in mitigating SSN in the whole power plane. From all above results,

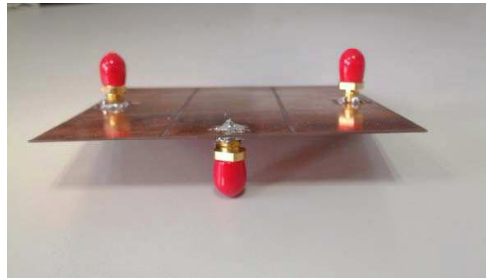
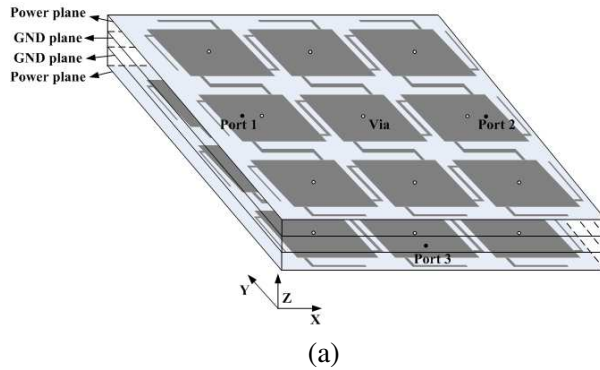


Figure 3. The test prototype of the novel vertical cascaded planar EBG structure. (a) The simulated model established in HFSS. (b) The real PCB for the proposed EBG.

the novel vertical cascaded planar EBG structure is proved to have excellent capability in suppressing SSN between power and ground plane.

3. THE EQUIVALENT CIRCUIT FOR THE PROPOSED STRUCTURE

Figure 5(a) shows the two ports are on the same power plane, and the equivalent circuit is shown in Figure 5(b). The circuit comprises three parts. The first part describes the equivalent capacitance C_{p1} and inductance L_p of the EBG patch. The second part describes equivalent capacitance C_{p2} between the neighboring unit cells and the bridge connecting the adjacent unit cells as the inductor L_b . The final part describes a through via connecting the power planes as the inductor L_v .

C_{p1} and L_p are illustrated in Eqs. (1) and (2) for the unit cell [14],

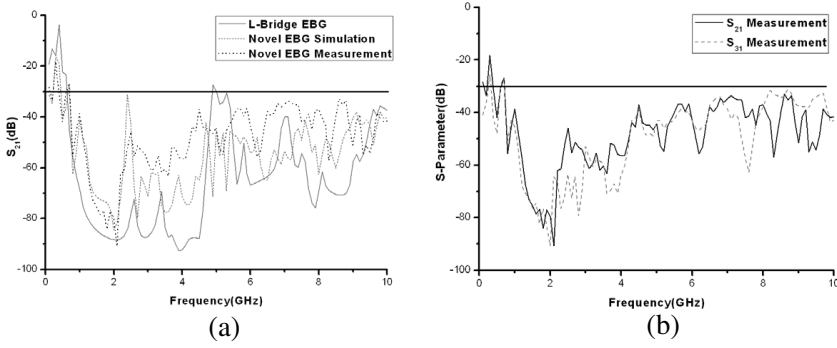


Figure 4. Simulated and measured insertion loss S -parameters for the novel vertical cascaded planar EBG structure. (a) The comparison of S_{21} between the L-Bridge board and the proposed design obtain by simulation and measurement. (b) The comparison of measured insertion loss including S_{21} and S_{31} for the proposed design.

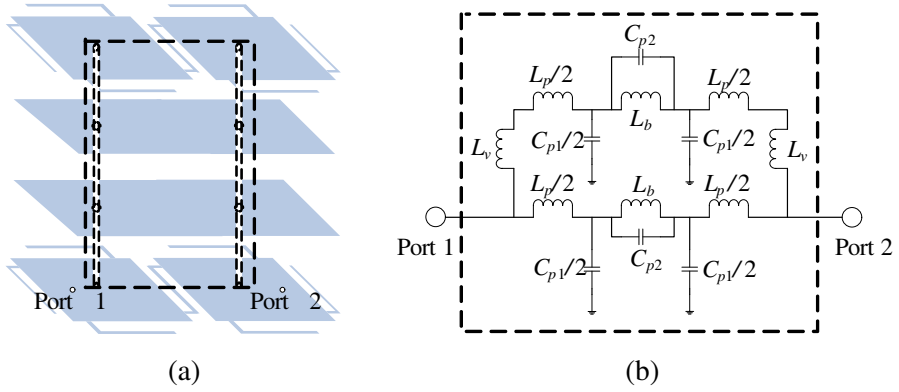


Figure 5. The equivalent circuit for the proposed structure. (a) The physics model. (b) The equivalent circuit model.

respectively.

$$C_{p1} = \epsilon_0 \epsilon_r \frac{w^2}{d} \quad (1)$$

$$L_P = \mu_0 d \quad (2)$$

where ϵ_r is the relative dielectric constant, w the length of unit cell, and d the thickness between the power plane and the ground plane. ϵ_0 and μ_0 are the permittivity and permeability of free space, respectively.

Equation (3) is used to calculate the gap capacitances between the patches [18].

$$C_{p2} = \frac{\varepsilon_0(1 + \varepsilon_r)w}{\pi} \cosh^{-1} \left(\frac{a}{g} \right) \quad (3)$$

where, g is the distance between the neighboring unit cells and a the cycle of the EBG structure, that $a = w + g$.

The L_b and L_v can be described as Eqs. (4) and (5) [5, 19], respectively.

$$L_b = lk \ln \left(2\pi \frac{d}{w_1} \right) \quad (4)$$

$$L_v = \mu_0 \frac{h_v}{2\pi} \left[\ln \left(\frac{2h_v}{r_v} + \sqrt{1 + \left(\frac{2h_v}{r_v} \right)^2} \right) - \sqrt{1 + \left(\frac{r_v}{2h_v} \right)^2} + \frac{r_v}{2h_v} + \frac{1}{4} \right] \quad (5)$$

where, $k = 0.2 \text{ nH/mm}$, l and w_1 are the length and width of the bridge between the neighboring unit cells, and h_v and r_v are the length and radius of the via.

It is necessary to estimate the bandwidth of the novel EBG structure. When the frequency is low, the impedance of C_{p2} is small as shown in Figure 5. So the circuit element C_{p2} can be ignored for analyzing the lower cut-off frequency.

According to Figure 5(b), the impedance of the circuit model is given by the following Equation (6).

$$\begin{aligned} Z_{in} &= 2 \left(\frac{j\omega L_p}{2} + \frac{2}{j\omega C_{p1}} // \frac{j\omega L_b}{2} \right) // 2 \left(j\omega L_v + \frac{j\omega L_p}{2} + \frac{2}{j\omega C_{p1}} // \frac{j\omega L_b}{2} \right) \\ &= \frac{[j\omega L_p (4 - \omega^2 L_b C_{p1}) + 4j\omega L_b]}{[(4 - \omega^2 L_b C_{p1})(2j\omega L_v + j\omega L_p) + 4j\omega L_b]} \\ &\quad \frac{[j\omega L_p (4 - \omega^2 L_b C_{p1}) + 4j\omega L_b]}{(4 - \omega^2 L_b C_{p1}) [4j\omega (L_b + L_p + L_v) - j\omega^3 L_b C_{p1} (L_p + L_v)]} \end{aligned} \quad (6)$$

According to the local resonance mechanism, Z_{in} is close to infinite when f is equal to f_L . Meanwhile, f_L needs to be selected a large value. So f_L is obtained by Equation (7).

$$f_L = \frac{1}{\pi} \sqrt{\frac{L_b + L_p + L_v}{L_b C_{p1} (L_p + L_v)}} \quad (7)$$

Similarly, the circuit element L_b can be ignored for analyzing the high cut-off frequency. According to Figure 5(b), the impedance of the

circuit model is given by the following Equation (8).

$$\begin{aligned} Z_{in} &= 2 \left[\frac{j\omega L_p}{2} + \frac{2}{j\omega(C_{p1} + C_{p2})} \right] // 2 \left[j\omega L_v + \frac{j\omega L_p}{2} + \frac{2}{j\omega(C_{p1} + C_{p2})} \right] \\ &= \frac{[4 - \omega^2 L_p(C_{p1} + C_{p2})] [4 - \omega^2(2L_v + L_p)(C_{p1} + C_{p2})]}{2j\omega(C_{p1} + C_{p2})[4 - \omega^2(L_v + L_p)(C_{p1} + C_{p2})]} \quad (8) \end{aligned}$$

By analyzing the circuit resonance on the circuit model and setting the image impedance to infinity, f_H is derived as Equation (9).

$$f_H = \frac{1}{\pi} \sqrt{\frac{1}{(L_v + L_p)(C_{p1} + C_{p2})}} \quad (9)$$

Based on planar EBG structure from above calculation, bandwidth BW can be obtained by Equation (10).

$$BW = f_H - f_L \quad (10)$$

Based on the above derivation, the vertical cascaded EBG structure can increase the length of the connecting bridge for reducing f_L and reduce the distance between the unit cells for increasing f_H in order to obtain the large bandwidth. It provides a method for increasing the bandwidth.

4. THE APPLICATION OF THE VERTICAL CASCADE

The vertical cascaded L-bridge EBG structure is present in the paper. If the plane at the bottom is replaced with the mender-line EBG structure, the vertical cascaded L-bridge and mender-line EBG structure can be achieved. Meanwhile, both the planes can also be replaced with the mender-line EBG structure. So these structures are simulated, and parameter S_{21} is shown in Figure 6. As shown in Figure 6, the lower cut-off frequency of the vertical cascaded EBG structure with both meander-lines is lower than the the one with one L-bridge and one meander-line at the restraining depth of -30 dB. The bandwidth is shown in Table 1. Because of the increase of the length of the bridge connection, the equivalent inductance L_b increases. In terms of Equation (7), the lower cut-off frequency will be reduced. Therefore, this structure increases the stop bandwidth.

In order to increase the stop bandwidth, the equivalent model of the circuit can be used to select different EBG structures to achieve vertical cascade. The proposed vertical cascade EBG not only raises the ability of SSN suppression to achieve the ultra-wideband, but also provides the method how to select the EBG structure to accomplish the vertical cascade.

Table 1. Suppressed behavior between comparison.

Cases	Suppression of the band gap depth at -30 dB	
	Frequency Range	Bandwidth
L-Bridge EBG	600 MHz–4.6 GHz	4 GHz
L-L EBG	710 MHz–10 GHz	9.29 GHz
L-M EBG	670 MHz–10 GHz	9.33 GHz
M-M EBG	610 MHz–10 GHz	9.39 GHz

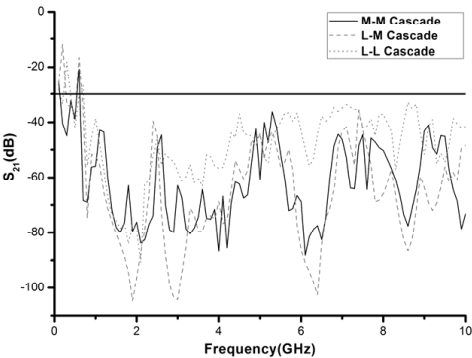


Figure 6. The comparison of S_{21} with the different EBG structures obtained by using vertical cascade.

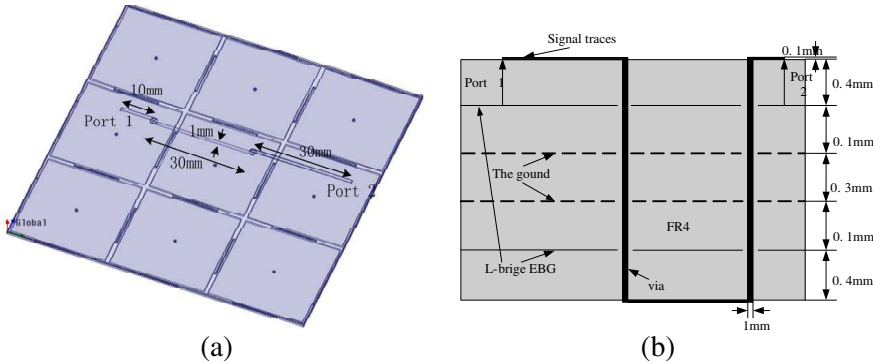


Figure 7. Six-layer PCB with signal layer referring to the proposed structure. (a) The three-dimensional view. (b) The side view.

5. THE ANALYSIS OF EYE DIAGRAM

The proposed vertical cascaded EBG structure shows good performance on SSN suppression, but time domain SI problems should also be considered in practical circuits. Therefore, simulated eye diagrams can be generated to analyze the SI issues. The maximum eye open (MEO) and maximum eye width (MEW) are used as metrics of the eye pattern quality [20].

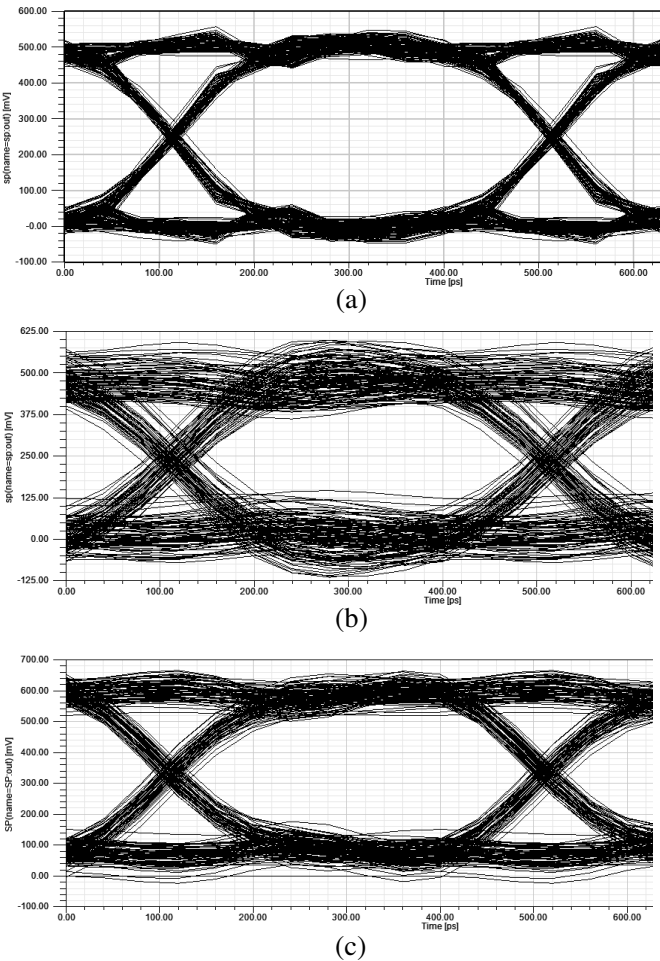


Figure 8. The simulated eye diagrams for the boards. (a) Reference board. (b) L-bridge EBG reference board. (c) Novel vertical cascaded EBG reference board.

As shown in Figure 7(a), the six-layer PCB is designed with the middle of the four planes, namely, power, ground, ground and power. The signal traces are designed as $50\ \Omega$ lines, which propagate along the traces on the top signal layer through via down to the bottom layer and back to the top layer again. The side view of PCB is shown in Figure 7(b).

Simulated eye diagrams can be generated by the Ansoft Designer. As shown in Figure 8, it can be seen that in the integrated power plane, $\text{MEO} = 400\text{ mV}$ and $\text{MEW} = 360\text{ ps}$, in the L-bridge EBG $\text{MEO} = 250\text{ mV}$ and $\text{MEW} = 300\text{ ps}$, and in the vertical cascaded L-bridge EBG, $\text{MEO} = 350\text{ mV}$ and $\text{MEW} = 340\text{ ps}$. Comparing the above results shows that the proposed structure possesses a better performance than the conventional L-bridge EBG in signal quality. However, there are some influences on the SI by using the proposed vertical cascaded EBG structure.

6. CONCLUSIONS

A novel vertical cascaded EBG structure is proposed in this paper to meet the requirement of the ultra-wideband SSN suppression. The stopband ranges from 710 MHz to 10 GHz at the restraining depth of -30 dB . The results of the test and simulation prove that the novel structure possesses a good performance in mitigating SSN. Simultaneously, the effect of stopband will be enhanced by using the different planar EBG structures to achieve vertical cascade. Moreover, the presented vertical cascaded EBG structure satisfies the requirements of SI in high-speed circuits. The novel planar EBG structures with the vertical cascaded method possess good performance providing a wide bandwidth for SSN suppression.

ACKNOWLEDGMENT

This work was partly supported by Key Lab of High-Speed Circuit Design and EMC, Ministry of Education, Xidian University of China (No. K505120206), by a research grant from the National Natural Science Foundation of China (No. 61106026) and the Fundamental Research Funds for the Central Universities of China.

REFERENCES

1. He, Y., L. Li, C. H. Liang, and Q. H. Liu, "EBG structures with fractal topologies for ultra-wideband ground bounce noise

- suppression,” *Journal of Electromagnetic Waves and Applications*, Vol. 24, No. 10, 1365–1374, 2010.
2. Yuan, C. P. and T. H. Chang, “Modal analysis of metal-stub photonic band gap structures in a parallel-plate waveguide,” *Progress In Electromagnetics Research*, Vol. 119, 345–361, 2011.
 3. Ding, T. H., Y. S. Li, D. C. Jiang, Y.-Z. Qu, and X. Yan, “Estimation method for simultaneous switching noise in power delivery network for high-speed digital system design,” *Progress In Electromagnetics Research*, Vol. 125, 79–95, 2012.
 4. Zhang, M. S., Y. S. Li, C. Jia, et al., “A power plane with wideband SSN suppression using a multi-via electromagnetic bandgap structure,” *IEEE Microwave and Wireless Components Letters*, Vol. 17, No. 4, 307–309, 2007.
 5. Shi, L. F., C. Meng, L. Y. Cheng, and C.-S. Cai, “Coplanar EBG structure with meander-L bridge for ultra-wideband mitigation of SSN,” *Journal of Electromagnetic Waves and Applications*, Vol. 26, Nos. 8–9, 1248–1260, 2012.
 6. Gao, M. J., L. S. Wu, and J. F. Mao, “Compact notched ultra-wideband bandpass filter with improved out-of-band performance using Quasi electromagnetic bandgap structure,” *Progress In Electromagnetics Research*, Vol. 125, 137–150, 2012.
 7. Chu, H., X. Q. Shi, and Y. X. Guo, “Ultra-wideband bandpass filter with a notch band using EBG array etched ground,” *Journal of Electromagnetic Waves and Applications*, Vol. 25, Nos. 2–3, 203–209, 2011.
 8. Gujral, M., J. L.-W. Li, T. Yuan, and C.-W. Qiu, “Bandwidth improvement of microstrip antenna array using dummy EBG pattern on feedline,” *Progress In Electromagnetics Research*, Vol. 127, 79–92, 2012.
 9. Kim, S. H., T. T. Nguyen, and J. H. Jang, “Reflection characteristics of 1-D EBG ground plane and its application to a planar dipole antenna,” *Progress In Electromagnetics Research*, Vol. 120, 51–66, 2011.
 10. Zhang, M. S., Y. S. Li, C. Jia, et al., “Simultaneous switching noise suppression in printed circuit boards using a compact 3-D cascaded electromagnetic-bandgap structure,” *IEEE Transactions on Microwave Theory and Techniques*, Vol. 55, No. 10, 2200–2207, 2007.
 11. Wu, T.-L., C.-C. Wang, Y.-H. Lin, et al., “A novel power plane with super-wideband elimination of ground bounce noise on high speed circuits,” *IEEE Microwave and Wireless Components Letters*, Vol. 15, No. 3, 174–176, 2005.

12. Qin, J. and O. M. Ramahi, "Ultra-wideband mitigation of simultaneous switching noise using novel planar electromagnetic bandgap structures," *IEEE Microwave and Wireless Components Letters*, Vol. 16, No. 9, 487–489, 2006.
13. Wang, X., B. Wang, Y. Bi, et al., "A novel uniplanar compact photonic bandgap power plane with ultra-broadband suppression of ground bounce noise," *IEEE Microwave and Wireless Components Letters*, Vol. 16, No. 5, 267–268, 2006.
14. Lin, D. B., K. C. Hung, C. T. Wu, and C.-S. Chang, "A serpent bridge electromagnetic bandgap structure for suppressing simultaneous switching noise," *Journal of Electromagnetic Waves and Applications*, Vol. 32, Nos. 2–3, 213–220, 2009.
15. Huang, C.-H. and T.-L. Wu, "Analytical design of via lattice for ground planes noise suppression and application on embedded planar EBG structures," *IEEE Transactions on Components, Packaging and Manufacturing Technology*, Vol. 3, No. 1, 21–30, 2013.
16. De Paulis, F., L. Raimondo, and A. Orlandi, "Impact of shorting vias placement on embedded planar electromagnetic bandgap structures within multilayer printed circuit boards," *IEEE Transactions on Microwave Theory and Techniques*, Vol. 52, No. 7, 1867–1876, 2010.
17. Li, J., J. Mao, S. Ren, and H. Zhu, "Embedded planar EBG and shorting via arrays for SSN suppression in multilayer PCBs," *IEEE Antennas and Wireless Propagation Letters*, Vol. 11, 1430–1433, 2012.
18. Kim, K. H. and J. E. S. Aine, "Analysis and modeling of hybrid planar-type electromagnetic-bandgap structures and feasibility study on power distribution network applications," *IEEE Transactions on Microwave Theory and Techniques*, Vol. 56, No. 1, 178–186, 2008.
19. Wang, T. K., C. Y. Hsieh, H. H. Chuang, et al., "Design and modeling of a stopband-enhanced EBG structure using ground surface perturbation lattice for power/ground noise suppression," *IEEE Transactions on Microwave Theory and Techniques*, Vol. 57, No. 8, 2047–2054, 2009.
20. Qin, J., O. M. Ramahi, and V. Granatstein, "Novel planar electromagnetic bandgap structures for mitigation of switching noise and EMI reduction in high-speed circuits," *IEEE Transactions on Electromagnetic Compatibility*, Vol. 49, 661–669, 2007.